International Journal of Greenhouse Gas Control 4 (2010) 537–545

Contents lists available at ScienceDirect

International Journal of Greenhouse Gas Control

journal homepage: www.elsevier.com/locate/ijggc

Mineral sequestration of carbon dioxide in basalt: A pre-injection overview of the CarbFix project

Sigurdur Reynir Gislason [a,*], Domenik Wolff-Boenisch [a], Andri Stefansson [a], Eric H. Oelkers [b], Einar Gunnlaugsson [c], Hólmfridur Sigurdardottir [c], Bergur Sigfusson [c], Wallace S. Broecker [d], Juerg M. Matter [d], Martin Stute [d], Gudni Axelsson [e], Thrainn Fridriksson [e]

[a] Institute of Earth Sciences, University of Iceland, Iceland
[b] CNRS/UMR 5563, Université Paul Sabatier, France
[c] Reykjavik Energy, Iceland
[d] Lamont-Doherty Earth Observatory, Columbia University, USA
[e] Iceland GeoSurvey, Reykjavík, Iceland

ARTICLE INFO

Article history:
Received 30 April 2009
Received in revised form 5 November 2009
Accepted 16 November 2009
Available online 22 January 2010

Keywords:
CO_2 fixation
CO_2 sequestration
Mineral carbonation
Mineral storage
Basalt carbonation
Dissolution rate

ABSTRACT

In this paper we describe the thermodynamic and kinetic basis for mineral storage of carbon dioxide in basaltic rock, and how this storage can be optimized. Mineral storage is facilitated by the dissolution of CO_2 into the aqueous phase. The amount of water required for this dissolution decreases with decreased temperature, decreased salinity, and increased pressure. Experimental and field evidence suggest that the factor limiting the rate of mineral fixation of carbon in silicate rocks is the release rate of divalent cations from silicate minerals and glasses. Ultramafic rocks and basalts, in glassy state, are the most promising rock types for the mineral sequestration of CO_2 because of their relatively fast dissolution rate, high concentration of divalent cations, and abundance at the Earth's surface. Admixture of flue gases, such as SO_2 and HF, will enhance the dissolution rates of silicate minerals and glasses. Elevated temperature increases dissolution rates but porosity of reactive rock formations decreases rapidly with increasing temperature. Reduced conditions enhance mineral carbonation as reduced iron can precipitate in carbonate minerals. Elevated CO_2 partial pressure increases the relative amount of carbonate minerals over other secondary minerals formed. The feasibility to fix CO_2 by carbonation in basaltic rocks will be tested in the CarbFix project by: (1) injection of CO_2 charged waters into basaltic rocks in SW Iceland, (2) laboratory experiments, (3) studies of natural analogues, and (4) geochemical modelling.

1. Introduction

The reduction of industrial CO_2 emissions is one of the main challenges of this century (e.g., Broecker, 2002, 2005, 2007, 2008; Hoffert et al., 2002; Lackner, 2003; Pacala and Socolow, 2004; Oelkers and Schott, 2005; Broecker and Kunzig, 2008; Oelkers and Cole, 2008). Among commonly proposed CO_2 storage techniques, the injection of anthropogenic CO_2 into deep geologic formations is quite promising due to their large potential storage capacity and geographic ubiquity (e.g., Bachu et al., 1994; Holloway, 2001; Metz et al., 2005; Oelkers and Cole, 2008; Benson and Cole, 2008). Carbon dioxide could be injected into deep geologic formations on land as a separate supercritical fluid. The effectiveness of this CO_2 storage and sequestration method depends strongly on the retention time, reservoir stability, and the risk of leakage (e.g., Hawkins, 2004; Rochelle et al., 2004; Benson and Cole, 2008). One way to enhance the long-term stability of injected CO_2 is through the formation of carbonate minerals. Carbonate minerals provide a long-lasting, thermodynamically stable, and environmentally benign carbon storage host. Mineral storage is in some cases the end product of geological storage of CO_2 (Metz et al., 2005; Benson and Cole, 2008). The degree to which mineral storage is significant and the rate at which mineralization occurs depend on the rock type and injection methods. Mineral carbonation of CO_2 could be enhanced by injecting it fully dissolved in water and/or by injection into silicate rocks rich in divalent metal cations such as basalts and ultramafic rocks.

2. *In situ* mineral sequestration

Mineral carbonation is the fixation of CO_2 as stable carbonate minerals, such as calcite ($CaCO_3$), dolomite ($CaMg(CO_3)_2$), magnesite

* Corresponding author at: Institute of Earth Sciences, University of Iceland, Sturlugata 7, 101 Reykjavik, Iceland. Tel.: +354 525 4497/252 4800; fax: +354 525 4499.
E-mail address: sigrg@raunvis.hi.is (S.R. Gislason).

1750-5836/$ – see front matter © 2009 Elsevier Ltd. All rights reserved.
doi:10.1016/j.ijggc.2009.11.013

($MgCO_3$), siderite ($FeCO_3$) and Mg–Fe carbonate solid solutions (Metz et al., 2005; Roger et al., 2006; Oelkers et al., 2008). *In situ* carbonation involves CO_2 injection into geologic formations while *ex situ* carbonation involves formation of CO_2 bearing minerals as part of an industrial process on the Earth's surface (Metz et al., 2005; Oelkers et al., 2008). Mineral carbonation requires combining CO_2 with metals to form carbonate minerals. With few exceptions, the required metals are divalent cations, including Ca^{2+}, Mg^{2+}, and Fe^{2+}. The most abundant cation sources for this process are silicate minerals and glasses. Field and experimental evidence suggests that the slowest and thus rate limiting step in mineral fixation of carbon in silicate rocks, such as basaltic rock, is the dissolution of the silicate minerals and glasses releasing the divalent cations. Natural waters in basaltic terrains and experimental solution in contact with basalt are typically saturated with respect to calcite at intermediate to high temperatures (Gislason and Arnórsson, 1990; Gislason et al., 1993).

After its injection into aquifers, CO_2 can dissolve in water, in accord with

$$CO_{2(g)} + H_2O = H_2CO_3 \quad (1a)$$

The product of this reaction, H_2CO_3 is aqueous carbonic acid, which can dissociate according to

$$H_2CO_3 = HCO_3^- + H^+ \quad (1b)$$

This reaction liberates protons causing the pH of the water to decrease. The pH of this solution will depend on the partial pressure of CO_2, temperature, alkalinity, and the salinity of the water. The pH of CO_2 saturated pure water, seawater, and the HN-1 groundwater to be used in the CarbFix project is shown in Table 1. The HN-1 groundwater is at 19 °C, but the same water is also modelled at 2 °C to underscore the effect of temperature on CO_2 solubility and pH. As shown in Table 1, CO_2 solubility increases, and thus the amount of water required for its dissolution decreases, with increasing CO_2 partial pressure, lower temperature, and lower salinity. At 25 bar CO_2 pressure, the water demand to fully dissolve the CO_2 is 27 tons of pure water for each ton of CO_2, but 31 tons of seawater are required at the same temperature and CO_2 pressure. At 19 °C, 22 tons of HN-1 water are required to fully dissolve CO_2 at 25 bar of pressure, but only 13 tons are required at 2 °C.

Basaltic rocks are rich in divalent cations such as Fe, Ca, and Mg. At low temperature and at neutral to high pH under oxidizing conditions, groundwaters in basaltic rocks are rich in divalent metal cations such as Ca^{2+} and Mg^{2+} (e.g., Gislason and Eugster, 1987a; Arnórsson et al., 2002; Flaathen et al., 2009). Under oxidizing conditions, Fe concentration is low, but its concentration can be elevated in reducing conditions. Dissolved metals could react with CO_2 to precipitate carbonate minerals according to

$$(Fe, Ca, Mg)^{2+} + CO_2 + H_2O = \underset{\text{carbonate minerals}}{(Fe, Ca, Mg)CO_3} + 2H^+ \quad (2)$$

Reaction (2) suggests that 2 moles of protons are produced for each mole of carbonate mineral produced. This reaction will only proceed to the right if the H^+ ions are consumed by a different reaction. These protons can be consumed by a variety of dissolution reactions in a basalt (Gislason and Eugster, 1987a,b;

Table 1
The solubility of dissolved inorganic carbon in water (DIC), pH and water demand to fully dissolve the CO_2 at variable partial pressure of CO_2, salinity and temperature. H_2O is pure water, average seawater composition is from Bruland (1983) and HN-1 is the groundwater to be used in the CarbFix project.

pCO_2 (bars)	H_2O (25 °C)			SEAWATER (25 °C)			HN-1 (19 °C)			HN-1 (2 °C)		
	In situ pH	DIC (mol/kg)	Water[a] demand	*In situ* pH	DIC (mol/kg)	Water[a] demand	*In situ* pH	DIC (mol/kg)	Water[a] demand	*In situ* pH	DIC (mol/kg)	Water[a] demand
0[b]	5.60	0.00002		8.22	0.002		8.90	0.002		9.13	0.002	
1	3.90	0.034	665	4.93	0.032	720	5.04	0.042	538	4.96	0.074	308
2	3.76	0.068	333	4.64	0.061	374	4.74	0.083	275	4.66	0.146	156
3	3.67	0.102	222	4.46	0.090	253	4.57	0.123	185	4.48	0.218	104
4	3.61	0.136	167	4.34	0.119	191	4.45	0.163	139	4.36	0.290	78
5	3.56	0.171	133	4.25	0.148	153	4.45	0.204	111	4.27	0.362	63
6	3.52	0.205	111	4.17	0.177	128	4.27	0.245	93	4.19	0.434	52
7	3.49	0.239	95	4.11	0.207	110	4.21	0.288	79	4.13	0.506	45
8	3.46	0.273	83	4.05	0.236	96	4.16	0.325	70	4.07	0.578	39
9	3.43	0.307	74	4.01	0.265	86	4.11	0.362	63	4.03	0.650	35
10	3.41	0.341	67	3.96	0.294	77	4.06	0.405	56	3.98	0.722	31
11	3.39	0.375	61	3.93	0.323	70	4.02	0.444	51	3.94	0.794	29
12	3.37	0.409	56	3.89	0.352	64	3.99	0.487	47	3.91	0.866	26
13	3.35	0.443	51	3.86	0.382	60	3.96	0.522	44	3.88	0.937	24
14	3.34	0.477	48	3.83	0.411	55	3.92	0.572	40	3.85	1.009	23
15	3.32	0.511	44	3.80	0.440	52	3.90	0.613	37	3.82	1.081	21
16	3.31	0.545	42	3.78	0.469	48	3.88	0.641	35	3.79	1.153	20
17	3.30	0.579	39	3.75	0.498	46	3.85	0.687	33	3.77	1.225	19
18	3.28	0.613	37	3.73	0.527	43	3.82	0.736	31	3.75	1.297	18
19	3.27	0.647	35	3.71	0.556	41	3.80	0.771	29	3.73	1.369	17
20	3.26	0.681	33	3.69	0.586	39	3.80	0.807	28	3.71	1.441	16
21	3.25	0.715	32	3.67	0.615	37	3.77	0.845	27	3.69	1.513	15
22	3.24	0.750	30	3.66	0.644	35	3.75	0.884	26	3.67	1.585	14
23	3.23	0.784	29	3.64	0.673	34	3.73	0.926	25	3.65	1.657	14
24	3.22	0.818	28	3.62	0.702	32	3.71	0.970	23	3.64	1.729	13
25	3.21	0.852	27	3.61	0.731	31	3.70	1.015	22	3.62	1.801	13
36	3.14	1.226	19	3.47	1.052	22	3.56	1.454	16	3.49	2.592	9
50	3.07	1.703	13	3.36	1.460	16	3.44	2.019	11			
55	3.05	1.873	12	3.33	1.606	14	3.40	2.220	10			
64	3.01	2.179	10	3.28	1.868	12						

[a] Minimum water demand, tons of water required to fully dissolve a ton of CO_2 at equilibrium.
[b] Initial partial pressure of the waters varies. In pure water it is atmospheric, 0.000385 bars, but less than atmospheric in the HN-1 groundwater. The modelling was done with the PHREEQC model using the PHREEQC.dat database (Parkhurst and Appelo, 1999).

Gislason and Arnórsson, 1990; Oelkers and Gislason, 2001; Gysi and Stefánsson, 2008; Matter et al., 2009) including

$$\underset{\text{Forsterite}}{Mg_2SiO_4} + 4H^+ \rightarrow 2Mg^{2+} + 2H_2O + SiO_{2(aq)} \quad (3)$$

$$\underset{\text{Ca-plagioclase}}{CaAl_2Si_2O_8} + 8H^+ \rightarrow Ca^{2+} + 2Al^{3+} + 2SiO_{2(aq)} + 4H_2O \quad (4)$$

and

$$\underset{\text{Basaltic glass}}{SiAl_{0.36}Ti_{0.02}Fe(III)_{0.02}Ca_{0.26}Mg_{0.28}Fe(II)_{0.17}Na_{0.08}K_{0.008}O_{3.36}} + 6.72H^+ = Si^{4+} + 0.36Al^{3+} + 0.02Ti^{4+} + 0.02Fe^{3+} + 0.17Fe^{2+} + 0.26Ca^{2+} + 0.28Mg^{2+} + 0.08Na^+ + 0.008K^+ + 3.36H_2O \quad (5)$$

The basaltic glass composition is that of Stapafell glass; this composition is very close to that of Mid Ocean Ridge Basalts (MORB) (Oelkers and Gislason, 2001; Gislason and Oelkers, 2003). In addition to advancing carbonate precipitation by proton consumption, reactions (3)–(5) also provide divalent metal cations to further promote this precipitation. The dissolution reactions (3)–(5) are fast compared with other silicate minerals with higher Si/O ratios such as Na-, and K-rich-feldspars and quartz (e.g., Oelkers and Schott, 1995; Oelkers, 2001b; Pokrovsky and Schott, 2000; Wolff-Boenisch et al., 2004a). As such, mafic and ultramafic rocks release divalent metals such as Ca at relatively rapid rates (Wolff-Boenisch et al., 2006). Consequently, *in situ* mineralization is believed to be effective in basalt or ultramafic rocks (e.g., McGrail et al., 2006; Matter et al., 2007; Kelemen and Matter, 2008).

There is diverse evidence demonstrating the potential of CO_2 sequestration in mafic and ultramafic rocks. First, despite the fact that less than 10% of the Earth's continental surface is covered by basalt (see Fig. 1), it takes up ~33% of all the CO_2 consumed in the form of alkalinity production during natural weathering of silicates at the Earth's surface (Dessert et al., 2003). Second, several well-documented examples of carbonation of basaltic rocks are known, such as through CO_2 metasomatism in a basalt-hosted petroleum reservoir (Roger et al., 2006), hydrothermal alteration (Arnórsson, 1989; Gudmundsson and Arnórsson, 2002; Neuhoff et al., 1999), and surface weathering of basalt (Gislason and Eugster, 1987a; Stefánsson and Gislason, 2001; Gislason et al., 1996, 2009; Flaathen et al., 2009). Third, enormous volumes of mafic and ultramafic rocks are present on the Earth's surface as shown for terrestrial basalt in Fig. 1. For example, the Columbia River basalts in the USA have a volume in excess of 200,000 km^3 and the Siberian basalts have a volume greater than 1,000,000 km^3. These large volumes have correspondingly large CO_2 sequestration capacities: McGrail et al. (2006) estimated that the Columbia River basalts alone have the capacity to sequester over 100 Gt of CO_2. In addition, low-permeability interbedded sediments and the impermeable massive basalt between the interflow zones provide a barrier for vertical CO_2 migration. Furthermore, Goldberg et al. (2008) demonstrated the large storage capacity of sub-oceanic basalt formations. Thus, storage in basalts is now considered to be among the most promising of the options for CO_2 storage (O'Connor et al., 2003; Oelkers et al., 2008).

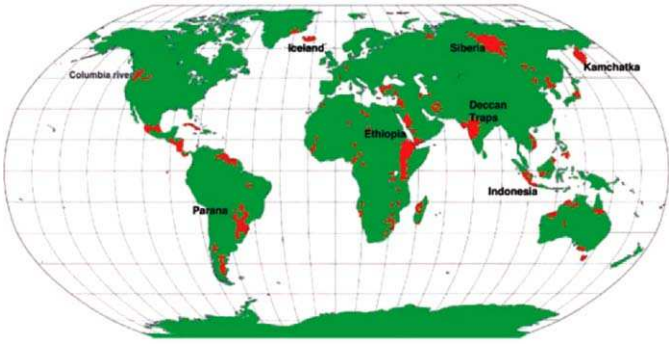

Fig. 1. Locations of terrestrial basalts that could serve as *in situ* mineral carbonation sites (from Oelkers et al., 2008).

The rock demand for mineral sequestration of carbon is large. It takes at least 5.9 tons of forsterite or 8.8 tons of basaltic glass to fix one ton of carbon, assuming that the mineral and glass dissolve completely and that all divalent cations end up in carbonates (Oelkers et al., 2008). As such one of the major challenges in mineral sequestration of CO_2 is to maximize the fraction of divalent cations that precipitate within carbonates versus other secondary minerals such as oxides, clays, and zeolites. Towards this goal injection systems need to be fine-tuned with respect to reactive surface areas, rate of injection and the partial pressure of CO_2.

2.1. Optimizing silicate rock dissolution rates

The availability of divalent metal cations for carbonate precipitation is enhanced by rapid dissolution rates of silicate rocks. These dissolution rates can be enhanced in several ways including choice of silicate rock, increasing the mineral-fluid interfacial surface area, and choice of temperature/injection fluid composition. These enhancement methods are described in detail below:

- *Crystallinity and rock composition* affect dissolution rates as demonstrated in Fig. 2 for the release rate of Ca^{2+} from silicates at 25 °C and pH of 4. Ultramafic and basaltic rocks such as gabbro and basaltic glass are rich in divalent cations and poor in silica; their dissolution rates are relatively fast, resulting in cation release rates that are about 2 orders of magnitude faster than that of granite and rhyolite. In addition, glassy rocks release Ca^{2+} about 2 times faster than their fully crystalline counterparts as shown in the figure (Wolff-Boenisch et al., 2006).
- *The mineral–fluid interfacial surface area* can be maximized by selecting porous rock formations and or causing hydro fracturing during CO_2 injection. In the vicinity of the injection wells, the CO_2 charged waters will be corrosive and dissolution will most likely create reactive surface area. However, as the reaction progresses downstream, secondary mineral formation could block the

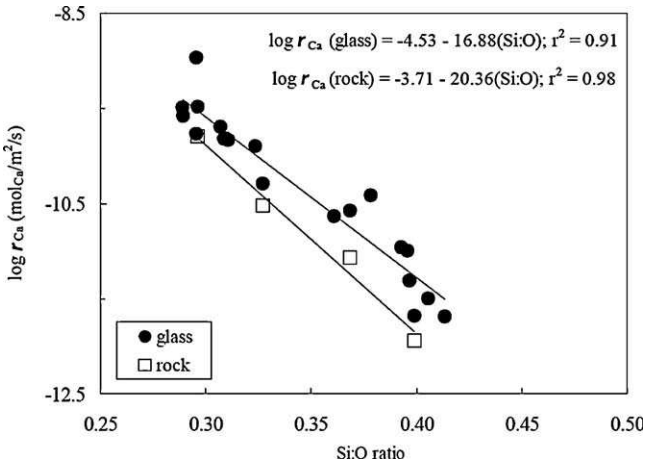

Fig. 2. Calculated Ca-release rates from the dissolution of granite, granodiorite, diorite, gabbro, and natural glasses in highly undersaturated solutions, normalized to geometric surface area at 25 °C and pH 4 (modified after Wolff-Boenisch et al., 2006).

reactive surface area, slowing dissolution of the primary rock (Cubillas et al., 2005; Stockmann et al., 2008).

- *Temperature/injection fluid composition* can be varied to optimize divalent cation release rates. The variation of basaltic glass dissolution rates as a function of temperature, solution composition, and saturation state can be described by (Daux et al., 1997; Oelkers, 2001a; Gislason and Oelkers, 2003):

$$r = A_A \exp\left(\frac{-E_A}{RT}\right)\left(\frac{a_{H^+}^3}{a_{Al^{3+}}}\right)^{1/3}\left(1-\exp\left(\frac{\Delta G_r}{\sigma RT}\right)\right) \quad (6)$$

where r denotes the geometric surface area normalized steady-state dissolution rate, a_i represents the activity of the subscripted aqueous species, A_A designates a pre-exponential factor equal to 2.5×10^{-6} mol of Si/cm^2/s, E_A refers to an activation energy equal to 25.5 kJ/mol, R stands for the gas constant, and T signifies the absolute temperature. According to Daux et al. (1997), the Temkin parameter, σ is equal to 1 when the hydrated basaltic glass layer is normalized to one Si atom, and ΔG_r refers to the Gibbs free energy of the reaction for the dissolution of the hydrated basaltic glass surface layer. The Temkin parameter represents the number of moles of precursor or activated complexes formed from one mole of the reacting mineral or glass as represented by its conventional stoichiometry. For example, the precursor complex for alkali-feldspar dissolution contains one Si atom, but the conventional formula for the alkali feldspars contains 3 Si (e.g., $KAlSi_3O_8$). Three moles of precursor or activated complexes are formed during the dissolution of an alkali feldspar and thus $\sigma = 3$ (Gautier et al., 1994).

Increasing temperature from 0 to 100 °C at pH 3.5, at fixed total concentration of dissolved aluminium (10^{-6} mol/kg), increases dissolution rates by a factor of 60. But the same temperature increase at pH 9 results in a 4.5 order of magnitude increase in rates. Temperature can be increased by increasing the depth of injection wells and or drilling into areas of high geothermal gradients. The disadvantage is that at high temperature the porosity of reactive rocks and therefore reactive surface area tend to decrease, and the solubility of carbon dioxide in water decreases with increasing temperature (e.g., Neuhoff et al., 1999; Table 1).

Fluid composition also affects rates. The higher the activity of protons (i.e., the lower the pH), the higher the dissolution rate. The pH also affects aqueous Al speciation. Its activity decreases faster than the 3rd power of the proton activity when the $Al(OH)_4^-$ becomes the dominating Al-species. This occurs at pH greater than about 7 depending on the temperature. As a result, basaltic glass dissolution rates increase with increasing pH at alkaline conditions (Eq. (6)). The far-from-equilibrium dissolution rates of basaltic glass and forsterite are compared as a function of pH at 25 and 30 °C in Fig. 3. The dissolution rate of forsterite decreases monotonically with increasing pH while the dissolution rate of basaltic glass shows a distinct minimum in the circum-neutral pH range before rising again at higher pH. The same applies also for crystalline basalt and feldspars (Gudbrandsson et al., 2008; Chou and Wollast, 1985). The pH of groundwaters in contact with basaltic glass and ultramafic rocks, sealed off from atmospheric CO_2 or other external CO_2 sources is high, ranging from 9 to 11 (Gislason and Eugster, 1987a,b; Gislason et al., 1996; Barnes and O'Neil, 1969; Kelemen and Matter, 2008; Alfredsson and Gislason, 2009). In contrast, water saturated at 25 bar pressure of CO_2 and 25 °C has $3.2 < pH < 4.0$ (Table 1). As can be seen in Fig. 3, decreasing pH from ~10 to 3.5 will increase forsterite dissolution rates by about 2 orders of magnitude, but will negligibly change basaltic glass dissolution rates.

Another method to enhance basaltic glass and feldspar dissolution rates is to add ligands that complex aqueous Al

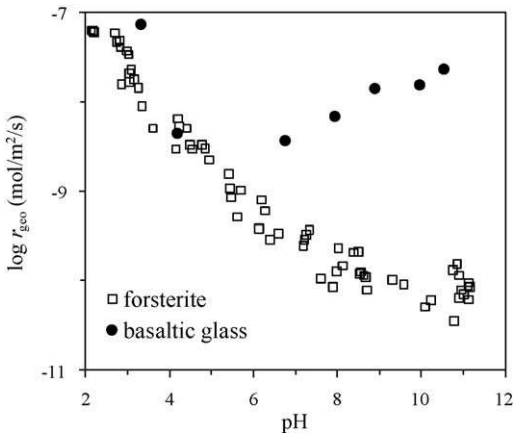

Fig. 3. Measured far-from-equilibrium dissolution rates of forsterite at 25 °C and of Stapafell basaltic glass at 30 °C, normalized to geometric surface area, as a function of pH. Data from Pokrovsky and Schott (2000) and Gislason and Oelkers (2003).

(Oelkers and Gislason, 2001; Harouiya and Oelkers, 2004; Wolff-Boenisch et al., 2004b; Flaathen et al., 2008). Flue gases from power plants and aluminium smelters commonly contain SO_2 and HF gases. These gas mixtures can be injected with the CO_2 to enhance the dissolution rates of Al–silicates. Sulphate (SO_4^{2-}) and fluoride (F^-) can complex Al^{3+} according to

$$Al^{3+} + SO_4^{2-} = Al(SO_4)^+ \quad (7)$$

$$Al^{3+} + F^- = AlF^{2+} \quad (8)$$

$$AlF^{2+} + F^- = AlF_2^+ \quad (9)$$

The formation of these complexes lowers aqueous Al^{3+} activity and enhances Al–silicate dissolution rates (Wolff-Boenisch et al., 2004b; Harouiya and Oelkers, 2004; Flaathen et al., 2008). The effect of fluoride (F^-) on basaltic glass dissolution rates is illustrated in Fig. 4. Rates increase by one order of magnitude in the presence of 100 μmol/kg total dissolved F in the pH range of 3–5.

CO_2 injection conditions can be fine-tuned such that most of the Al released by dissolution of Al silicates forms insoluble Al–Si phases and Fe^{2+} does not oxidize. This prevents the slowdown of the primary Al–silicate dissolution rates due to increasing aqueous Al^{3+} activity and prevents the formation of secondary mineral formation containing the divalent cations, or their oxidized ions, aimed for carbonate precipitation. Minerals that could consume

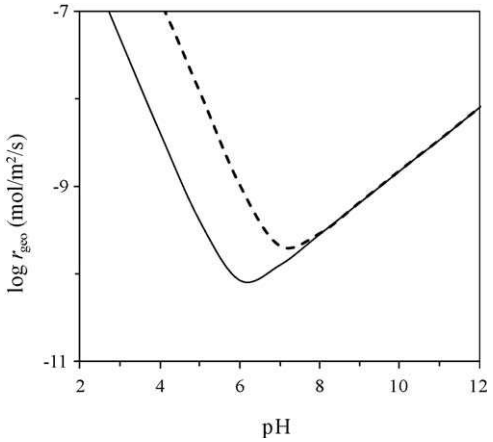

Fig. 4. Modelled far-from-equilibrium basaltic glass (48 wt% SiO_2) dissolution rates, normalized to geometric surface area, as a function of pH at 25 °C, 10^{-6} M Al_{total}, with (hatched curve) and without 10^{-4} M F_{total} concentrations (modified after Wolff-Boenisch et al., 2004b).

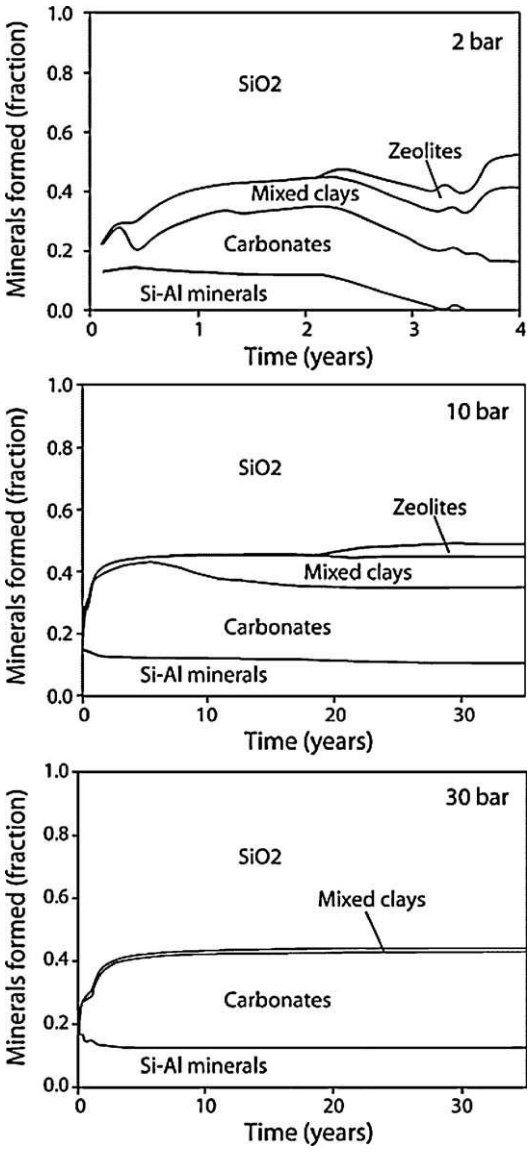

Fig. 5. Mole fractions of secondary minerals formed as a function of reaction progress for groundwater in contact with basaltic glass saturated at 25 °C with 2, 10, and 30 bars CO_2. Mixed clays include celadonite, Ca–Fe–Mg smectites, and chlorites. Carbonates include calcite, dolomite, siderite, magnesite, and Mg–Fe carbonate. Si–Al minerals include allophanes, imogolite, and kaolinite (from Gysi and Stefánsson, 2008).

these divalent and trivalent cations include iron and manganese oxy-hydroxides, smectites, and zeolites. Model calculations suggest that elevated partial pressure of CO_2 will enhance the efficiency of the system as shown in Fig. 5 (Gysi and Stefánsson, 2008). The higher the partial pressure of CO_2 the higher the fraction of released divalent cations precipitating in carbonates.

3. The CarbFix project

The CarbFix project has been created to develop and optimize practical and cost-effective technology for *in situ* carbon mineralization in basalts. CarbFix includes field scale injection of CO_2 charged waters into basaltic rocks, laboratory experiments, studies of natural analogues, and state of the art geochemical modelling. The project was established by Icelandic, French, and American scientists and was officially launched in 2007. The main partners in the project are Reykjavik Energy, University of Iceland, The Earth Institute at Columbia University in New York, and the Centre National de la Recherche Scientifique/Université Paul Sabatier in France.

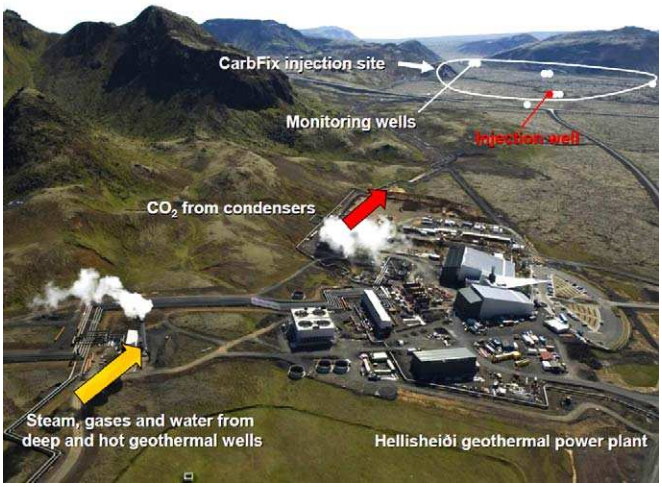

Fig. 6. Aerial photograph of the Hellisheidi geothermal power plant and the CarbFix injection site which includes an injection and several monitoring wells. The geothermal power plant as a source of the CO_2 is approximately 3 km to the north of the injection site. The moss covered post-glacial basaltic lava flows cover the ground in the upper right part of the figure. The hill to the left of the power plant is a hyaloclastite (broken glass) ridge. This formation is mostly basaltic glass, formed under glacier during the last glaciations.

The CarbFix injection site is located about 3 km south of the Hellisheidi geothermal power plant in SW Iceland (see Figs. 6 and 7). The geothermal power plant currently produces up to 60,000 tons of CO_2 per year; this production will increase as the plant expands. This CO_2 gas is a by-product of the geothermal energy production. The gas originates from magma situated at few km depth. The geothermal steam originates from the geothermal system and contains less than 1 wt% of geothermal gases as shown at the bottom of Table 2 (Stefánsson and Fridriksson, 2007). The composition of the gas varies with time, depending on which wells are in use. CO_2 concentrations in the steam range from 60 to over 100 mmol/kg, with average gas mole fractions of close to 0.6. This steam also contains important quantities of other gases including H_2S, H_2 and N_2.

Plans call for the complete dissolution of CO_2 in water during injection, resulting in a single fluid phase entering the rock. Water for this injection will be obtained from well HN-1 (Fig. 7). CO_2 will be dissolved into this water as it is injected into well HN-2 at 25 bar pressure at about 350 m depth. The water level in HN-2 is at about 100 m depth. The dissolution of carbon dioxide in water at Hellisheidi is limited by the poor solubility of H_2 and N_2 in water. These gases will contribute 83–92% of the total gas pressure at 25–75 °C, whereas CO_2 will contribute only 6–15% of the total gas pressure (Stefánsson and Fridriksson, 2007). The dissolution of this mixture of gases would require an unpractical amount of water as shown in Table 1. Therefore, the various geothermal gases will be separated in a pilot gas processing plant. The gases from the power plant will be compressed and cooled. H_2S will be separated from the CO_2 and re-injected with the spent geothermal water into deep geothermal reservoirs. Once separated from other gases, the amount of water required to dissolve CO_2 depends on the temperature and CO_2 partial pressure as described above (see also Table 1).

4. Geology and pre-injection characterization of the Hellisheidi injection site

The rocks at the Hellisheidi site are of ultrabasic to basaltic composition (~45 to 49% SiO_2) and are both glassy and crystalline

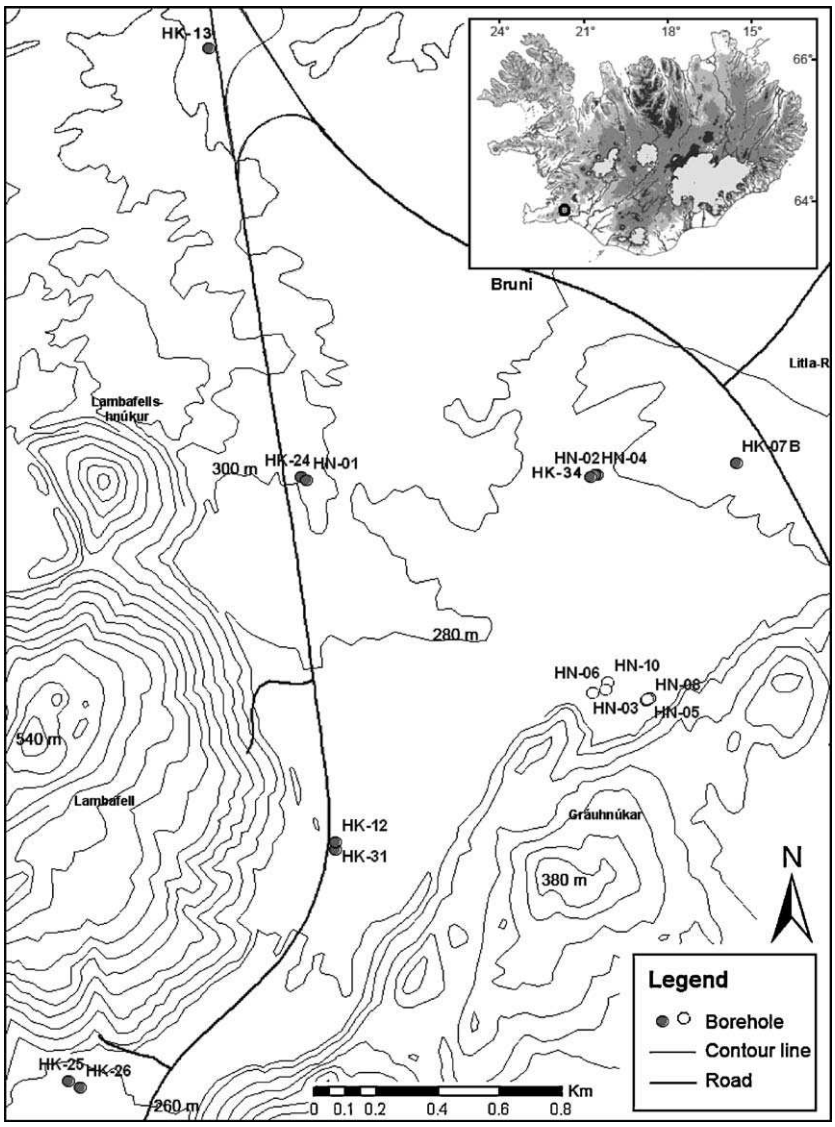

Fig. 7. A map of the Hellisheidi injection site in SW-Iceland. Wells used by the CarbFix project are marked with gray dots (modified from Alfredsson et al., 2008).

Table 2
Gas concentrations and mole fractions in steam at Turbines 1 and 2 at the Hellisheidi Power Plant[a].

	Turbine 1 06-5101[b] (mmol/kg)	Turbine 1 05-5102 (mmol/kg)	Turbine 1 average mole fraction	Turbine 2 06-5107 (mmol/kg)	Turbine 2 05-5112 (mmol/kg)	Turbine 2 average mole fraction
CO_2	103.044	102.693	0.625	59.808	60.122	0.559
H_2S	32.629	32.178	0.197	27.047	26.976	0.252
H_2	25.826	26.47	0.159	17.813	18.057	0.167
N_2	2.834	2.62	0.017	1.803	2.153	0.018
CH_4	0.22	0.246	0.0014	0.209	0.196	0.0019
O_2 + Ar	0.231	0.188	0.0013	0.104	0.218	0.0015
Total non-H_2O gas in steam wt%	0.579	0.575		0.364	0.367	

[a] Analyses provided by Reykjavík Energy.
[b] 06-5101 was collected on 28/10/06 at 11.10 a.m.–11.47 a.m.; 06-5102 was collected on 28/10/06 at 13.28 a.m.–14.02 a.m.; 06-5107 was collected on 02/11/06 at 10.56 a.m.–11.38 a.m.; 06-5112 was collected on 02/11/06 at 13.30 a.m.–14.05 a.m.

(Alfredsson et al., 2008). The majority of the rocks are of olivine tholeiite composition. The crystalline lava flows on the surface were formed after the last glaciations and are covered with moss (post-glacial lava flows; right part of Fig. 6) but glassy ridges, referred to as hyaloclastites (broken glass; upper left in Fig. 6), were formed under ice during the last glaciation 11,500–110,000 y ago (Saemundsson, 1980; Alfredsson et al., 2008). The magma that formed the hyaloclastite ridges was quenched in the meltwater at the eruption site, forming glass, crystalline rock fragments and pillow lavas (e.g., Jones, 1969; Schopka et al., 2006). The mountains seen in Figs. 6 and 7 are hyaloclastite ridges but the flat lowland is covered with lava flows. A cross-section of the

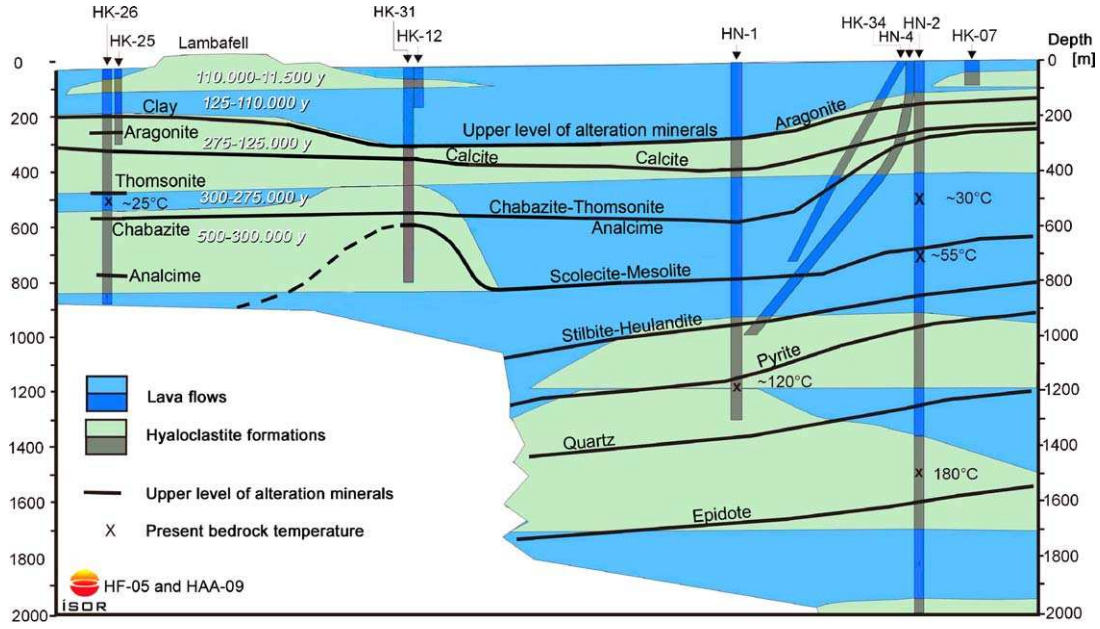

Fig. 8. NE–SW cross-section of the lithology at the CarbFix injection site. Boreholes are marked as columns. The first appearance of alteration minerals with depth is depicted as black curves labelled with the mineral name. Estimated ages of the rock formations for the first 800 m are shown in the upper left of the section (modified from Alfredsson et al., 2008).

injection site, from north east to south west together with the location of injection and monitoring wells are shown in Fig. 8.

The youngest rock formations are the lavas enclosing the Lambafell hyaloclastite ridge (Figs. 7 and 8) and are 2000–5000 year old. Temperature, age and alteration of the rocks increase with depth. The target injection formation is at 400–800 m depth consisting of basaltic lavas and hyaloclastite, with calcite and Ca-zeolites as common alteration minerals (Alfredsson et al., 2008). The temperature at the injection depth interval is between 30 and 50 °C. Some of the observation wells cut into the target injection reservoir, whereas others are shallow wells in the near-surface aquifer (Fig. 8).

Prior to CO_2 injection, which is scheduled to start early 2010, a pre-injection field study was completed. Various methods have been applied since 2007; including systematic monitoring of groundwater chemistry, soil CO_2 flux measurements, and borehole geophysical measurements. In addition, two tracer tests have been conducted within the injection reservoir.

The waters in the shallow aquifer above 400 m depth are at 8–12 °C and are oxygen-rich. These waters have a pH between 7.7 and 8.4, have an *in situ* partial pressure of CO_2 that is close to atmospheric CO_2 pressure and are undersaturated with respect to calcite. The deeper wells are cased down to 400 m and extend down to 800–2000 m as shown in Fig. 8. The most productive aquifers are within the first 150 m below the casing. The waters from the deeper wells are at 18–33 °C and are oxygen poor. The pH of these waters ranges from 8.4 to 9.4, the partial pressure of CO_2 is below that of the atmosphere and the waters are at saturation with calcite, a common secondary mineral in the rocks (Alfredsson and Gislason, 2009).

Diffuse CO_2 degassing has been measured on fresh snow by a closed chamber method at selected sites within the injection area. The results are shown in Fig. 9. The measurements were performed on a 25 m by 25 m grid concentrated around the HN-2 injection well, the HN-4 and HK-34 monitoring wells (see Figs. 6–9), and on four traverses across the Threngsli valley, downstream from the injection site. The total number of measurements was 284. The average and uniform flux was around 3 $gCO_2/m^2/day$, corresponding to about 1000 tons of CO_2 per year from each square kilometer. The maximum flux was about 20 $gCO_2/m^2/day$ but values higher than 10 $gCO_2/m^2/day$ were observed in only 5 locations. The average diffuse CO_2 flux in the Threngsli valley was similar, albeit slightly lower than what has been observed from vegetated soil that is not affected by

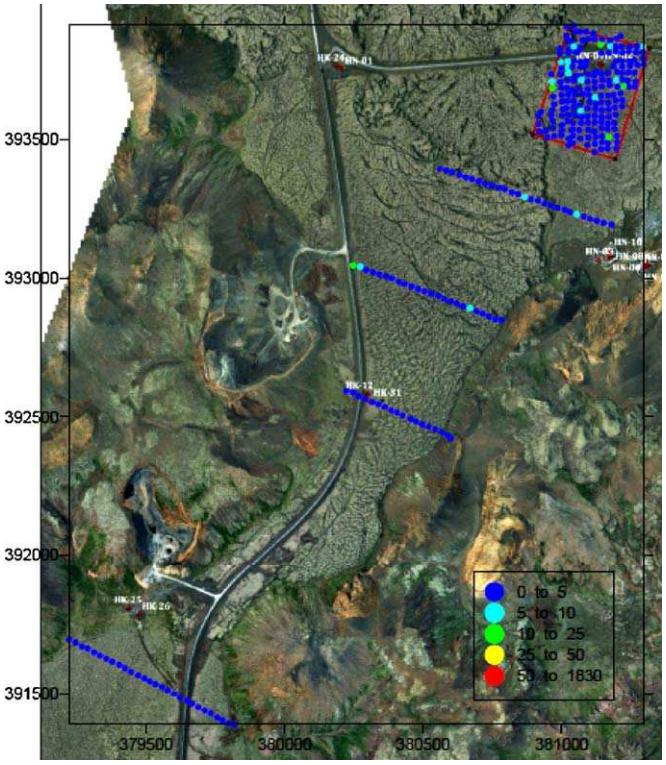

Fig. 9. Arial photo of the CarbFix injection site at Hellisheidi. The soil degassing sample spots are superimposed on the figure. The colour of the spots indicates the flux from 0 to 1830 $gCO2/m^2/day$. The sample spots are concentrated around the injection well (HN-2) and the first two monitoring wells (HN-4 and HK-34). The flux is uniform with few excursions. The average flux is 3 $gCO_2/m^2/day$.

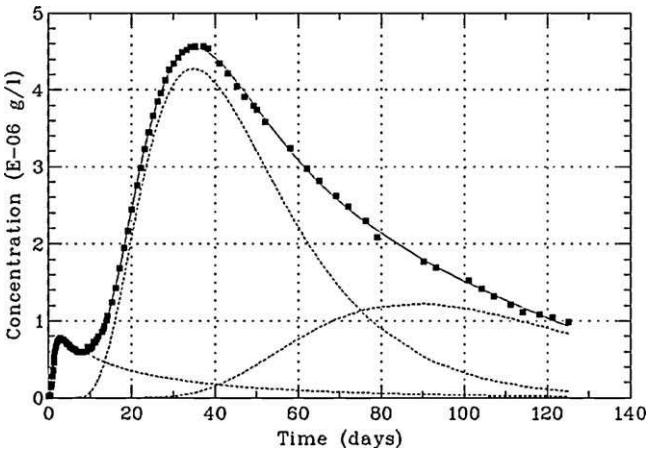

Fig. 10. Observed (filled squares) and simulated Na-fluorescein concentration in observation well HN-4. The simulated recovery curves assume three distinct flow paths. The sum of the three channels fits the measured concentrations well; the coefficient of determination is 96.8% (modified from Khalilabad et al., 2008).

geothermal degassing at Reykjanes (4.1 gCO_2/m^2/day; Fridriksson et al., 2006) and Krafla (6 gCO_2/m^2/day; Ármannsson et al., 2007).

A tracer test, using Na-fluorescein as a conservative tracer, was carried out from November 2007. In addition, a large scale tracer test with sulphur hexafluoride (SF_6) and Na-fluorescein is ongoing since June 2008. The preliminary tracer test was conducted as a forced gradient test between two adjacent wells, HN-2 and HN-4 (note that well HN-4 is tilted; see Figs. 7 and 8). A flow field between the two wells was induced by continuous injection of water at a rate of 5 kg/s in well HN-2 and pumping of water at a rate of 10 kg/s from well HN-4. Operation of this doublet commenced 3 days prior to tracer injection to develop a steady-state flow field. A half a kilo of Na-fluorescein dye was then released as a slug into well HN-02 (Axelsson, 2007; Khalilabad et al., 2008). The distance between the two wells is 60 m at 400 m depth and 360 m at 600 m depth. A one-dimensional dispersion transport process was assumed to interpret the data as shown in Fig. 10. This model neglects diffusion, adsorption, and retardation (Axelsson et al., 2005). The preliminary tracer test revealed preferential flow paths within the target reservoir, as reflected by the first peak in Fig. 10, but that most of the basaltic bedrock consists of a relatively homogeneous porous media (Axelsson, 2007; Khalilabad et al., 2008). This interconnected porous media may provide high tortuosity and large reactive surface area promoting CO_2–water–rock interaction.

5. The CO_2 injection pilot study

Plans call for an initial test injection of 0.07 kg/s of CO_2 dissolved in 2 kg/s of water at 19 °C. This translates to 2.2 thousand tons of CO_2 per year. If successful, the experiment will be up-scaled. Conservative tracers, such as trifluormethyl sulphur pentafluoride (SF_5CF_3), and amidorhodamine G fluoresceint dye will be mixed into the injected gas and water stream to monitor the subsurface transport. As an additional constraint on the carbonate mass balance, ^{14}C labelled CO_2 will be added to the injection water. The CO_2 gas will be pumped into injection well HN-2, at about 25 bar total pressure and 350 m depth. The water stream will carry CO_2 bubbles down-well to more than 500 m depth where the hydrostatic pressure is over 40 bars, ensuring complete dissolution of the CO_2 before entering the aquifer. The pH of the water after dissolution at 25 bar *in situ* partial pressure of CO_2 is estimated to be 3.7 and the dissolved inorganic carbon concentration (DIC) is estimated to be ~1 mol/kg as shown in Table 1. Prior to water rock interactions, most DIC will be in the form of dissolved carbonic acid (H_2CO_3) whereas only a trivial amount of bicarbonate (HCO_3^-) will form. As the CO_2 charged waters percolate through the rock the dissolution of mafic minerals and glass will consume the protons provided by the carbonic acid. As a result of these dissolution reactions, combined with dilution and dispersion the pH of the injected water will rise and alkalinity will increase. Concomitantly, the concentration of dissolved elements will increase and alteration minerals will form, resulting in mineral fixation of carbon as suggested by Eq. (2) and Fig. 5.

Mineral precipitation may eventually clog pores in the host basalt. The target zone is more than 2 km long, 1000 m wide, and 500 m thick as shown in Figs. 7 and 8. This is at least one cubic km of basalt. Assuming 10% porosity of the rocks, of which only 10% will eventually be filled with calcite, yields a 0.01 km^3 volume for calcite precipitation. This volume can accommodate 12 million tons of CO_2. At the present CO_2 emission rate of magmatic CO_2 from the geothermal power plant at Hellisheidi Iceland (60,000 tons/year), it would take about 200 years to fill this available pore space.

6. Conclusions

The thermodynamic and kinetic basis for mineral storage of carbon dioxide in basaltic rock is described in this paper, and how this storage can be optimized. Mineral storage is facilitated by the dissolution of CO_2 gas into the aqueous phase. The water density increases, once the gas is fully dissolved, minimizing its tendency to flow towards the Earth's surface. The feasibility to fix CO_2 by carbonation in basaltic rocks will be tested by its injection into basaltic rock at the Hellisheidi site south-west Iceland in the year 2010.

Acknowledgements

We would like to thank all the graduate students that are working within the CarbFix project: Helgi Alfredsson, Edda Sif Aradóttir, Therese Flaathen, Iwona M. Galeczka, Snorri Gudbrandsson, Alexander Gysi, Mahnaz Rezvani Khalilabad, Elísabet V. Ragnheidardóttir, Diana Fernandez de la Reguera and Gabrielle J. Stockmann. We are grateful to colleagues and friends that have helped with the project, in particular Eydís S. Eiríksdóttir, Teitur Gunnarsson, Húni Sighvatsson, Claus Ballzus, Einar Örn Þrastarson, Gretar Ívarsson, Gestur Gíslason, Guðmundur Lárusson, Grímur Björnsson, Björn Hardarson, Klaus Lackner, Susanne Stipp and Andrew Putnis. Furthermore we would like to express our gratitude to the president of Iceland Ólafur Ragnar Grímsson, and his staff members Örnólfur Thorsson, Kristján Gay Burgess, and Árni Sigurjónsson for their support. The CarbFix project is funded by, Reykjavík Energy, The Environmental and Energy Research Fund of Reykjavík Energy, European Commission Marie Curie Grants (MRTN-2006-31482 and PITN-GA-2008-215360), Icelandic Science Foundation (RANNIS-071017) and University of Iceland (Tækjakaupasjódur).

References

Alfredsson, H.A., Hardarson, B.S., Franzson, H., Gislason, S.R., 2008. CO_2 sequestration in basaltic rock at the Hellisheidi site in SW Iceland: stratigraphy and chemical composition of the rocks at the injection site. Miner. Mag. 72, 1–5.

Alfredsson, H.A., Gislason, S.R., 2009. CarbFix—CO_2 sequestration in basaltic rock: chemistry of the rocks and waters at the injection site, Hellisheidi, SW-Iceland. Geochim. Cosmochim. Acta 73 (Suppl. 1), A28.

Ármannsson, H., Fridriksson, T., Wiese, F., Hernandez, P., Perez, N., 2007. CO_2 budget of the Krafla geothermal system, NE-Iceland. In: Bullen, T.D., Wang, Y. (Eds.), Water–Rock Interaction. Taylor & Francis Group, London, pp. 189–192.

Arnórsson, S., 1989. Deposition of calcium carbonate minerals from geothermal waters—theoretical considerations. Geothermics 18, 33–40.

Arnórsson, S., Gunnarsson, I., Stefánsson, A., Andrésdóttir, A., Sveinbjörnsdóttir, A.E., 2002. Major element chemistry of surface- and ground waters in basaltic

terrain, N-Iceland. I. Primary mineral saturation. Geochim. Cosmochim. Acta 23, 4015–4046.
Axelsson, G., Björnsson, G., Montalvo, F., 2005. Quantitative interpretation of tracer test data. In: Horne, R., Okandan, E. (Eds.), Proceedings of the World Geothermal Congress, Antalya, Turkey.
Axelsson, G., 2007. Characterizing an intermediate depth target zone for CO_2 injection in the Hellisheiði area—points concerning tracer selection and tracer test execution. Icelandic GeoSurvey Report, Reykjavik, Iceland.
Bachu, S., Gunter, W.D., Perkins, E.H., 1994. Aquifer disposal of CO_2: hydrodynamic and mineral trapping. Energy Convers. Mgmt. 35, 269–279.
Barnes, I., O'Neil, J.R., 1969. The relationship between fluids in some fresh Alpine-type ultramafics and possible modern serpentinization. West. United States Geol. Soc. Bull. 80, 1947–1960.
Benson, S.M., Cole, D.R., 2008. CO_2 sequstration in deep sedimentary formations. Elements 4, 325–331.
Broecker, W.S., 2002. Carbon futures. Geosphere-Biosphere Interactions and Climate 66–80.
Broecker, W.S., 2005. Global warming: take action or wait? Jökull 55, 1–16.
Broecker, W.S., 2007. Climate change: CO_2 arithmetic. Science 315, 1371–11371.
Broecker, W.S., 2008. CO_2 capture and storage: possibilities and perspectives. Elements 4, 295–297.
Broecker, W.S., Kunzig, R., 2008. Fixing Climate: What Past Climate Changes Reveal About the Current Threat—An How to Counter It. Hill and Wang, New York.
Bruland, K.W., 1983. Trace elements in sea water. In: Riley, J.P., Chester, R. (Eds.), Chemical Oceanography, vol. 8. Academic Press, London, pp. 157–220.
Chou, L., Wollast, R., 1985. Steady state kinetics and dissolution mechanisms of albite. Am. J. Sci. 285, 963–993.
Cubillas, P., Köhler, S., Prieto, M., Oelkers, E.H., 2005. Experimental determination of the dissolution rates of calcite, aragonite and bivalves. Chem. Geol. 216, 59–77.
Daux, V., Guy, D., Advocat, T., Crovisier, J.L., Stille, P., 1997. Kinetic aspects of basaltic glass dissolution at 90 °C: role of aqueous silicon and aluminium. Chem. Geol. 142, 109–126.
Dessert, C., Dupré, B., Gaillardet, J., Francois, L.M., Allégre, C.J., 2003. Basalt weathering laws and the impact of basalt weathering on the global carbon cycle. Chem. Geol. 202, 257–273.
Flaathen, T.K., Oelkers, E.H., Gislason, S.R., 2008. The effect of aqueous sulphate on basaltic glass dissolution rates. Miner. Mag. 72, 39–41.
Flaathen, T.K., Oelkers, E.H., Gislason, S.R., Sveinbjörnsdóttir, A.E., 2009. Chemical evolution of the Mt. Hekla, Iceland, groundwaters: a natural analogue for CO_2 sequestration in basaltic rocks. Appl. Geochem. 24, 463–474.
Fridriksson, T., Kristjansson, B.R., Ármannsson, H., Margretardóttir, E., Ólafsdottir, S., Chiodini, G., 2006. CO_2 emissions and heat flow through soil, fumaroles, and steam heated mud pools at the Reykjanes geothermal area, SW Iceland. Appl. Geochem. 21, 1551–1569.
Gislason, S.R., Eugster, H.P., 1987a. Meteoric water-basalt interactions. II. A field study in N.E. Iceland. Geochim. Cosmochim. Acta 51, 2841–2855.
Gislason, S.R., Eugster, H.P., 1987b. Meteoric water–basalt interactions. I. A laboratory study. Geochim. Cosmochim. Acta 51, 2827–2840.
Gislason, S.R., Arnórsson, S., 1990. Saturation state of natural waters in Iceland relative to primary and secondary minerals in basalts. In: Spencer, R.J., Chou, I.-M. (Eds.), Fluid–Mineral Interactions: A Tribute to Geochemical Society. Special Publication No. 2, pp. 373–393.
Gislason, S.R., Veblen, D.R., Livi, K.J.T., 1993. Experimental meteoric water–basalt interactions: characterization and interpretation of alteration products. Geochim. Cosmochim. Acta 57, 1459–1471.
Gislason, S.R., Arnórsson, S., Ármannsson, H., 1996. Chemical weathering of basalt in SW Iceland: effects of runoff, age of rocks and vegetative/glacial cover. Am. J. Sci. 296, 837–907.
Gislason, S.R., Oelkers, H.E., 2003. The mechanism, rates and consequences of basaltic glass dissolution. II. An experimental study of the dissolution rates of basaltic glass as a function of pH and temperature. Geochim. Cosmochim. Acta 67, 3817–3832.
Gislason, S.R., Oelkers, E.H., Eiriksdottir, E.S., Kardjilov, M.I., Gisladottir, G., Sigfusson, B., Snorrason, A., Elefsen, S.O., Hardardottir, J., Torssander, P., Oskarsson, N., 2009. Direct evidence of the feedback between climate and weathering. Earth Planet. Sci. Lett. 277, 213–222.
Goldberg, D.S., Takahashi, T., Slagle, A.L., 2008. Carbon dioxide sequestration in deep-sea basalt. Proc. Nat. Acad. Sci. 105, 9920–9925.
Gudbrandsson, S., Wolff-Boenisch, D., Gislason, S.R., Oelkers, E.H., 2008. Dissolution rates of crystalline basalt at pH 4 and 10 and 25°–75 °C. Miner. Mag. 72, 155–158.
Gudmundsson, B., Arnórsson, S., 2002. Geochemical monitoring of the Krafla and Námafjall geothermal areas, N-Iceland. Geothermics 31, 195–243.
Gautier, J.-M., Oelkers, E.H., Schott, J., 1994. Experimental study of K-feldspar dissolution rates as a function of chemical affinity at 150 °C and pH 9. Geochim. Cosmochim. Acta 58, 4549–4560.
Gysi, A.P., Stefánsson, A., 2008. Numerical modeling of CO_2–water–basalt interaction. Miner. Mag. 72, 55–59.
Harouiya, N., Oelkers, E.H., 2004. An experimental study of the effect of aqueous fluoride on quartz and alkali-feldspar dissolution rates. Chem. Geol. 205, 155–167.
Hawkins, D.G., 2004. No exit: thinking about leakage from geologic carbon storage sites. Energy 29, 1571–1578.
Hoffert, M.I., Caldeira, K., Benford, G., Criswell, D.R., Green, C., Herzog, H., Jain, A.K., Kheshgi, H.S., Lackner, K.S., Lewis, J.S., Lightfoot, H.D., Manheimer, W., Mankins, J.C., Mauel, M.E., Perkins, L.J., Schlesinger, M.E., Volk, T., Wigley, T.M.L., 2002. Advanced technology paths to global climate stability: energy for a greenhouse planet. Science 298, 981–987.
Holloway, S., 2001. Storage of fossil fuel-derived carbon dioxide beneath the surface of the earth. Ann. Rev. Energy Environ. 26, 145–166.
Jones, J.G., 1969. Intraglacial volcanoes of the Laugarvatn region, south-west Iceland. I. Q. J. Geol. Soc. London 124, 197–211.
Khalilabad, M.R., Axelsson, G., Gislason, S.R., 2008. Aquifer characterization with tracer test technique; permanent CO_2 sequestration into basalt. SW Iceland. Min. Mag. 72, 121–125.
Kelemen, P., Matter, J.M., 2008. In situ carbonation of peridotite for CO_2 storage. Proc. Nat. Acad. Sci. 105, 17295–17300.
Lackner, K.S., 2003. A guide to CO_2 sequestration. Science 300, 1677–1678.
Matter, J.M., Takahashi, T., Goldberg, D., 2007. Experimental evaluation of in situ CO_2-water-rock reactions during CO_2 injection in basaltic rocks. Implications for geological CO_2 sequestration. Geochem. Geophys. Geosyst. 8 , doi:10.1029/2006GC001427.
Matter, J.M., Broecker, W.S., Stute, M., Gislason, S.R., Oelkers, E.H., Stefánsson, A., Wolff-Boenisch, D., Gunnlaugsson, E., Axelsson, G., Björnsson, G., 2009. Permanent Carbon Dioxide Storage into Basalt: The CarbFix Pilot Project, Iceland. Energy Procedia 1 (1), 3641–3646.
McGrail, B.P., Schaef, H.T., Ho, A.M., Chien, Y.J., Dooley, J.J., Davidson, C.L., 2006. Potential for carbon dioxide sequestration in flood basalts. J. Geophys. Res. 111, B12201.
Metz, B., Davidson, O., de Coninck, H., Loos, M., Meyer, L. (Eds.), 2005. IPCC Special Report on Carbon Dioxide Capture and Storage. Cambridge University Press, New York.
Neuhoff, P.S., Fridriksson, T., Arnorsson, S., Bird, D.K., 1999. Porosity evolution and mineral paragenesis during low-grade metamorphism of basaltic lavas at Teigarhorn, Eastern Iceland. Am. J. Sci. 299, 467–501.
O'Connor, W.K., Rush, G.E., Dahlin, D.C., 2003. Laboratory studies on the carbonation potential of basalt: applications to geological sequestration of CO_2 in the Columbia River Basalt Group. In: AAPG Annual Meeting Expanded Abstracts, vol. 12, pp. 129–130.
Oelkers, E.H., 2001a. A general kinetic description of multi-oxide silicate mineral and glass dissolution. Geochim. Cosmochim. Acta 65, 3703–3719.
Oelkers, E.H., 2001b. An experimental study of forsterite dissolution rates as a function of temperature and aqueous Mg and Si concentration. Chem. Geol. 175, 485–494.
Oelkers, E.H., Gislason, S.R., 2001. The mechanism, rates, and consequences of basaltic glass dissolution. I. An experimental study of the dissolution rates of basaltic glass as a function of aqueous Al, Si, and oxalic acid concentration at 25°C and pH = 3 and 11. Geochim. Cosmochim. Acta 65, 3671–3681.
Oelkers, E.H., Schott, J., 2005. Geochemical aspects of CO_2 sequestration. Chem. Geol. 217, 183–186.
Oelkers, E.H., Cole, D.R., 2008. Carbon dioxide sequestration. A solution to a global problem. Elements 4, 305–310.
Oelkers, E.H., Gislason, S.R., Matter, J., 2008. Mineral carbonation of CO_2. Elements 4, 331–335.
Oelkers, E.H., Schott, J., 1995. Experimental study of anorthite dissolution and the relative mechanism of feldspar hydrolysis. Geochim. Cosmochim. Acta 59, 5039–5053.
Pacala, S., Socolow, R., 2004. Stabilization wedges: solving the climate problem for the next 50 years with current technologies. Science 305, 968–971.
Parkhurst, D.L., Appelo, C.A.J., 1999. User's guide to PHREEQC (Version 2)—a computer program for speciation, batch-reaction, one-dimensional transport, and inverse geochemical calculations. U.S.G.S. Water-Resources. Inv. Report 99-4259.
Pokrovsky, O.S., Schott, J., 2000. Kinetics and mechanism of forsterite dissolution at 25 °C and pH from 1 to 12. Geochim. Cosmochim. Acta 64, 3313–3325.
Roger, K.L., Neuhoff, P.S., Pedersen, A.K., Bird, D.K., 2006. CO_2 metasomatism in a basalt-hosted petroleum reservoir, Nuussuaq, West Greenland. Lithos 92, 55–82.
Rochelle, C.A., Czernichowski-Lauriol, I., Milodowski, A.E., 2004. The impact of chemical reactions on CO_2 storage in geological formations: a brief review. Geol. Soc. London Spec. Publ. 233, 87–106.
Saemundsson, K., 1980. Outline of the geology of Iceland. Jökull 29, 7–28.
Schopka, H.H., Gudmundsson, M.T., Tuffen, H., 2006. The formation of Helgafell, southwest Iceland, a monogenetic subglacial hyaloclastite ridge: sedimentology, hydrology and volcano–ice interaction. J. Volcanol. Geotherm. Res. 152, 359–377.
Stockmann, G., Wolff-Boenisch, D., Gislason, S.R., Oelkers, E.H., 2008. Dissolution of diopside and basaltic glass: the effect of carbonate coating. Miner. Mag. 72, 135–139.
Stefánsson, A., Gislason, S.R., 2001. Chemical weathering of basalts, SW Iceland: effect of rock crystallinity and secondary minerals on chemical fluxes to the ocean. Am. J. Sci. 301, 513–556.
Stefánsson, A., Fridriksson, T.H., 2007. Solubility of Hellisheidi geothermal gases in water. Internal Report to Reykjavík Energy. Icelandic Geosurvey, Reykjavik.
Wolff-Boenisch, D., Gislason, S.R., Oelkers, E.H., Putnis, C.V., 2004. The dissolution rates of natural glasses as a function of their composition at pH 4 and 10.6, and temperatures from 25 to 74 °C. Geochim. Cosmochim. Acta 68, 4843–4858.
Wolff-Boenisch, D., Gislason, S.R., Oelkers, E.H., 2004. The effect of fluoride on the dissolution rates of natural glasses at pH 4 and 25 °C. Geochim. Cosmochim. Acta 68, 4571–4582.
Wolff-Boenisch, D., Gislason, S.R., Oelkers, E.H., 2006. The effect of crystallinity on dissolution rates and CO_2 consumption capacity of silicates. Geochim. Cosmochim. Acta 70, 858–870.